Journal of Sound and Vibration (2001) **248**(3), 477–497
doi:10.1006/jsvi.2001.3824, available online at http://www.idealibrary.com on IDEAL®

FREE VIBRATIONS OF CIRCULAR CYLINDRICAL SHELLS WITH AN INTERIOR PLATE USING THE RECEPTANCE METHOD

Y.-S. LEE AND M.-H. CHOI

Department of Mechanical Design Engineering, Chungnam National University, 220 *Gung-Dong, Yuseong, Daejeon* 305-764, *Korea. E-mail:yslee@shell.cnu.ac.kr*

(*Received* 23 *October* 2000, *and in final form* 2 *April* 2001)

This paper describes the method to analyze the free vibrations of simply supported cylindrical shells with an interior rectangular plate by using the receptance method. This method is based on the ratio of a deflection (or slope) response to a harmonic force (or moment) at the joint. After finding the free vibrational characteristics of the simply supported plate and shell before combination, the frequency equation of the combined system is obtained by considering the continuity conditions at the joint between the plate and the shell. When the line load and moment applied along the joint are assumed as the Dirac delta and sinusoidal function, the continuity conditions at the joint are proven to be satisfied. The numerical results are compared with published works and experimental results in order to show the validity of the formulation, and that the analytical results agree with those from other methods.

1. INTRODUCTION

In many industrial applications, the beams, plates and shells are often used as basic components of the structures. Especially, the circular cylindrical shells are used to approximate more complex structures such as in aerospace, submarine and nuclear engineering. But actual structures in the engineering field are combinations of basic structural elements. Compared to the cylindrical shell, the combined shell with a longitudinal, interior rectangular plate seems to be a more realistic model. For example, an aircraft fuselage with floor structure may be idealized as a combined shell of the plate and shell. When the plate and shell are combined, the dynamic behavior of the combined structure becomes relatively complicated due to the mechanical coupling between the interior plate and the shell. Thus, it is necessary to develop an analytical method of evaluating the vibrational characteristics and to obtain information about the vibrations of the combined shell.

There are many studies in the literature for the free vibration of basic elements such as the plate and shell. Among available papers, Leissa [1, 2] investigated extensively the vibration of the plate and shell with various shapes and boundary conditions, and offered to engineers useful information for the design of structures. Sewall *et al.* [3, 4] applied the Rayleigh–Ritz method to solve for the natural frequencies and mode shapes of stiffened shells, circular and non-circular shells. Lee and Kim [5, 6] studied the influence of various boundary conditions on the free vibrational behavior of the rotating composite cylindrical shells with axial and circumferential stiffeners. They used Love's shell theory based on the discrete stiffener theory to derive the governing equation of the stiffened shell. One useful approach for

0022-460X/01/480477 + 21 $35.00/0

analyzing the free vibration of combined structures is the receptance method discussed by Bishop and Johnson [7]. Sakharov [8] applied the receptance method to calculate the vibrational characteristics of a shell system composed of a circular cylindrical shell with an annular plate at one end. Azimi *et al.* [9, 10] studied the natural frequencies and modes of continuous rectangular plates and cylindrical polygonal ducts using the receptance method. Huang and Soedel [11] presented the results of an analysis of both ends of a simply supported cylindrical shell with a plate at an arbitrary axial position. Also Yim *et al.* [12] applied this method to analyze the free vibration of a clamped–free circular cylindrical shell with a plate attached at an arbitrary axial position. They obtained the frequency equation of the combined system by considering the continuity condition at the shell/plate joint, numerical results compared with these from a finite element analysis and vibration test.

Although the receptance method is not applied in the analysis of the vibration for combined structures of the interior rectangular plate and cylindrical shell, which can be idealized in the aircraft fuselage or submarine structure, several methods are used to treat combined shell problems with an interior rectangular plate. Peterson and Boyd [13], who used a Rayleigh–Ritz method to study the free vibration of a circular cylindrical shell partitioned by an interior rectangular plate, developed the first analytical approach. This paper presented the effects of several parameters such as joint conditions between the plate and the shell, thickness of the structure and the position of the plate on the frequencies and the mode shapes of the combined shell. Irie *et al.* [14, 15] studied the free vibration of non-circular cylindrical shells with longitudinal interior partitions and jointed conical–cylindrical shells by using the transfer matrix. Langley [16] applied a dynamic stiffness technique for the vibration analysis of a simply supported stiffened shell structure. Recently, Missaoui *et al.* [17] studied the free and forced vibration of a cylindrical shell with a floor partition based on a variational formulation in which the structural coupling is simulated using artificial spring systems. Petyt and Wei [18] presented an efficient analytical model of an idealized fuselage structure or predicting vibrational characteristics by using an extended Rayleigh–Ritz technique. They considered a circular cylindrical stiffened shell and a rectangular sandwich plate with equally spaced stiffeners for the fuselage and floor respectively.

In the present study, the receptance method is employed to obtain the vibrational characteristics of a simply supported cylindrical shell with an interior plate. For the individual system of the simply supported plate and shell, the natural frequencies and mode shape functions are obtained through the Rayleigh–Ritz procedure based on the energy principle. The analytical results are compared with those of the existing literature and an experiment using the modal testing [19]. The analytical results agreed well with those from the available results and the test showing the validity of the current formulation.

2. ANALYTICAL FORMULATION

The geometry of the circular cylindrical shell with an interior plate and the co-ordinate systems are shown in Figure 1. The displacement components of the shell and the plate in each direction are presented as u_1^s, u_2^s, u_3^s and u_1^p, u_2^p, u_3^p respectively, where, superscript s and p indicate the shell and the plate respectively. The plate is attached at θ_1^* and θ_2^* position of the shell based on the vertical centerline.

2.1. FREE VIBRATION OF THE SHELL AND THE PLATE

It is necessary that the natural frequencies of the component systems before combination are calculated to obtain the vibrational characteristics of the combined system. For a plate

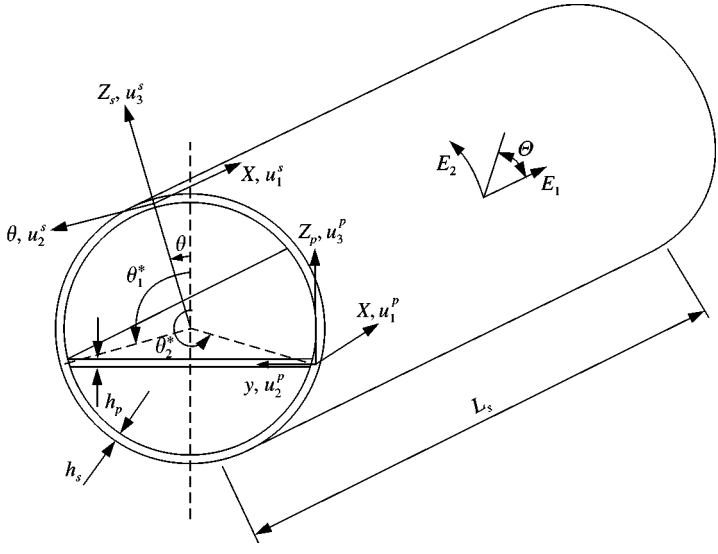

Figure 1. Geometry of the circular composite cylindrical shell with an interior plate.

simply supported along all edges, it has been shown in reference [20] that the solution of the equation of motion of the transverse vibration of the plate can be expressed as

$$u_3^p(x, y, t) = U_{3mn}^p(x, y)\mathrm{e}^{\mathrm{j}\omega_{mn}t}$$

$$= \sum_{m=1}^{m^*}\sum_{n=1}^{n^*} A_{mn}\sin\frac{m\pi x}{L_p}\sin\frac{n\pi y}{b}\mathrm{e}^{\mathrm{j}\omega_{mn}t}, \tag{1}$$

where A_{mn} are the undetermined coefficients and ω_{mn} are the angular natural frequencies as [21]

$$\omega_{mn} = \frac{\pi^2}{L_p^2\sqrt{\rho_p}}\sqrt{D_{11}m^4 + 2(D_{12} + 2D_{66})m^2n^2R^2 + D_{22}n^4R^4}, \tag{2}$$

where R is the plate aspect ratio (L_p/b) and D_{ij} ($i, j = 1, 2, 6$) are the bending stiffness. The transverse mode shapes corresponding to those frequencies are

$$U_{3mn}^p(x, y) = \sin(m\pi x/L_p)\sin(n\pi y/b), \quad m, n = 1, 2, 3, \ldots. \tag{3}$$

Similarly, the natural frequencies and mode shape functions of the simply supported cylindrical shell are obtained to apply the receptance method for the combined structure. These are calculated by Rayleigh–Ritz method based on the energy principle and Love's shell theory. For the symmetric laminates with multiple specially orthotropic layers, the strain and kinetic energy of the laminated shell as given in reference [22] can be written as

$$U_s = \frac{1}{2}\int_0^{L_s}\int_0^{2\pi}[A_{11}\varepsilon_x^2 + 2A_{12}\varepsilon_x\varepsilon_\theta + A_{22}\varepsilon_\theta^2 + A_{66}\varepsilon_{x\theta}^2$$

$$+ D_{11}\kappa_x^2 + 2D_{12}\kappa_x\kappa_\theta + D_{22}\kappa_\theta^2 + D_{66}\kappa_{x\theta}^2]a\,\mathrm{d}\theta\,\mathrm{d}x \tag{4}$$

and

$$T_s = \frac{1}{2}\int_0^{L_s}\int_0^{2\pi} \rho_{st}[(\dot{u}_1^s)^2 + (\dot{u}_2^s)^2 + (\dot{u}_3^s)^2]\, a\, \mathrm{d}\theta\, \mathrm{d}x, \tag{5}$$

where a is the radius of the cylindrical shell.

The strain–displacement relations for a circular cylindrical shell are based on Love's shell theory. They can be expressed as follows:

$$\varepsilon_x = \mathrm{u}_{1,x}^s, \quad \varepsilon_\theta = \frac{1}{a}(u_{2,\theta}^s + u_3^s), \quad \varepsilon_{x\theta} = \frac{1}{a}\ u_{1,\theta}^s + u_{2,x}^s, \tag{6}$$

$$\kappa_x = -\,u_{3,xx}^s, \quad \kappa_\theta = -\frac{1}{a^2}(u_{3,\theta\theta}^s - u_{2,\theta}^s), \quad \kappa_{x\theta} = -\frac{1}{a}(2u_{3,x\theta}^s - u_{2,x}^s). \tag{7}$$

where (,) represents partial differentiation for the space and ε, κ are the mid-surface strains and curvatures respectively.

The displacement functions which satisfy the boundary conditions at both ends are of the form

$$\begin{Bmatrix} u_1^s \\ u_2^s \\ u_3^s \end{Bmatrix} = \sum_{m=1}^{m^*}\sum_{n=1}^{n^*} \begin{Bmatrix} U_{1mn}\cos(m\pi x/L_s)\cos n(\theta-\phi) \\ U_{2mn}\sin(m\pi x/L_s)\sin n(\theta-\phi) \\ U_{3mn}\sin(m\pi x/L_s)\cos n(\theta-\phi) \end{Bmatrix} \mathrm{e}^{\mathrm{i}\omega_{mn}t}, \tag{8}$$

where U_{imn} are the undetermined amplitude coefficients, ϕ is the phase angle, and m, n represent half wave numbers in the axial and circumferential directions respectively. Substituting equations (6–8) into the energy equations (4–5) and solving the minimization problem relative to the undetermined coefficients by applying the Rayleigh–Ritz method, the frequency equation of a simply supported cylindrical shell can be obtained as follows:

$$|k_{ij} - \omega_{mn}^2 m_{ij}| = 0, \quad i,j = 1,2,3, \tag{9}$$

where ω_{mn} are the angular natural frequencies of the shell. The three natural modes that are associated with the natural frequencies at each m, n combination can be expressed as

$$\begin{Bmatrix} u_{1mn}^s \\ u_{2mn}^s \\ u_{3mn}^s \end{Bmatrix} = \begin{Bmatrix} U_{1mn}^s/U_{3mn}^s\cos(m\pi x/L_s)\cos n(\theta-\phi) \\ U_{2mn}^s/U_{3mn}^s\sin(m\pi x/L_s)\sin n(\theta-\phi) \\ \sin(m\pi x/L_s)\cos n(\theta-\phi) \end{Bmatrix}. \tag{10}$$

2.2. DISPLACEMENTS AND SLOPES DUE TO DYNAMIC LOADING

Figure 2 shows the cross-sectional view of the displacements and the slopes at shell/plate junctions due to the dynamic transverse line loads and moments around the shell exerted by the motion of vibration. The displacements of a structure subjected to dynamic loading can be expressed by modal displacement and modal participation factor as an infinite series:

$$u_i(x,\theta,t) = \sum_{m=1}^{\infty}\sum_{n=1}^{\infty} \eta_{mn}(t)\, U_{imn}(x,\theta), \quad i = 1,2,3, \tag{11}$$

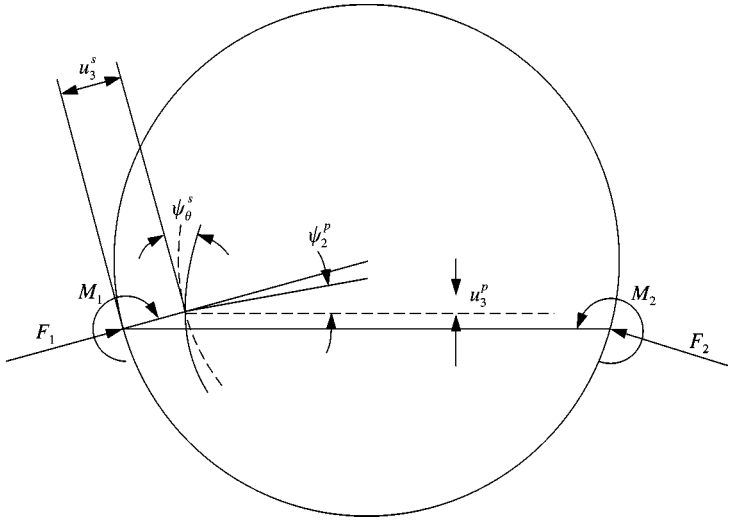

Figure 2. Loads (or moments) and displacements (or slopes) of the combined structure.

where U_{imn} denote the mode components of the plate and the shell in three principal directions, mn represents the mode number. Also, the modal participation factor η_{mn} is the root of the following modal equation for the steady state harmonic response of the structure:

$$\ddot{\eta}_{mn} + 2\zeta_{mn}\omega_{mn}\dot{\eta}_{mn} + \omega_{mn}^2\eta_{mn} = F_{mn}^* e^{j\omega t}, \tag{12}$$

where

$$\varsigma_{mn} = \lambda/2\rho h\omega_{mn}, \tag{13}$$

$$F_{mn}^* = \frac{1}{\rho h N_{mn}} \int_0^{2\pi} \int_0^{L_s} q_i^* U_{imn}\, a\, dx\, d\theta, \tag{14}$$

$$N_{mn} = \int_0^{2\pi} \int_0^{L_s} U_{mn}^2 a\, dx\, d\theta. \tag{15}$$

ς_{mn} is the modal damping coefficient, and λ is the damping factor. The input forcing functions, q_i^* $(i = 1, 2, 3)$ are the forces applied at two joints in the axial, circumferential and transverse normal direction. In equation (12), the mode participation factor of more mn can be obtained as

$$\eta_{mn} = \frac{F_{mn}^*}{\omega_{mn}^2\sqrt{[1-(\omega/\omega_{mn})^2]^2 + 4\zeta_{mn}^2(\omega/\omega_{mn})^2}} e^{j\omega t}. \tag{16}$$

Thus, if we take mn terms of the modal expansion series as approximation to an infinite number, we can present the displacement in terms of the mode summation. By neglecting the damping of the system, the displacements of the structure in equation (11) can be rewritten as

$$u_i(x, \theta, t) = \sum_{m=1}^{\infty} \sum_{n=1}^{\infty} \frac{F_{mn}^*}{(\omega_{mn}^2 - \omega^2)} U_{imn}(x, \theta) e^{j\omega t}. \tag{17}$$

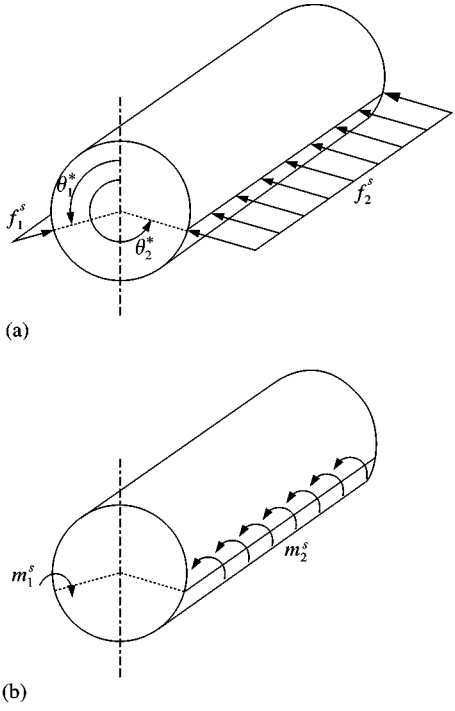

Figure 3. Forces (a) and moments (b) applied on the shell at the joints.

ω_{mn} is the angular frequency of two independent systems which are calculated by Love's shell theory and classical plate theory. The dynamic forcing function F_{mn}^* can be obtained in equation (14), and the displacements of the plate and shell in equation (17) will be used later to calculate the receptances.

When a rectangular plate is attached at (x, θ_1^*) and (x, θ_2^*) positions of the cylindrical shell, the transverse dynamic excitation exerted at the joints due to the constraint of the displacements of the shell by the plate is shown in Figure 3(a). In this case the line loads on a cylindrical shell can be assumed as

$$q_3^*(x, \theta^*, t) = f_i^*(x, \theta^*, t) = F_i^s \sin(\bar{m}\pi x/L_s)\delta(\theta - \theta_i^*)e^{j\omega t}, \quad i = 1, 2, \tag{18}$$

where δ is the Dirac delta function. Also, f_1^*, f_2^* are the transverse forcing functions applied at two joints in the circumferential direction. The transverse mode shape of the shell satisfying the simply supported boundary conditions is used as equation (19) by neglecting the components in axial and circumferential directions in equation (10).

$$U_{3mn}^s = \sin(m\pi x/L_s)\cos(n\theta). \tag{19}$$

Substituting equations (18) and (19) into equation (14), in the case of $\bar{m} = m$ the dynamic forcing function F_{mn}^* is found to be

$$F_{mn}^* = F_{mn}^*|_{F_1} + F_{mn}^*|_{F_2}, \tag{20}$$

where

$$F^*_{mn}|_{F_1} = \frac{F^s_1 L_s}{2\rho_s h_s N_{mn}} \cos n\theta^*_1, \qquad F^*_{mn}|_{F_2} = \frac{F^s_2 L_s}{2\rho_s h_s N_{mn}} \cos n\theta^*_2. \tag{21}$$

$F^*_k|_{F_1}$ is the dynamic forcing function with only F_1 applied and $F^*_k|_{F_2}$ is the one with only F_2 applied, and in equation (15) N_{mn} is given as

$$N_{mn} = L_s a\pi/2. \tag{22}$$

Using equations (17) and (20), the dynamic displacement of the shell can be expressed as

$$u^s_3(x, \theta, t) = u^s_3(x, \theta, t)|_{F_1} + u^s_3(x, \theta, t)|_{F_2}, \tag{23}$$

where

$$u^s_3(x, \theta, t)|_{F_1} = \frac{F^s_1 L_s}{2\rho_s h_s N_{mn}} \sum_{m=1}^{\infty} \sum_{n=1}^{\infty} \frac{\cos n\theta^*_1}{(\omega^2_{mn} - \omega^2)} \sin(m\pi x/L_s) \cos n\theta e^{j\omega t}, \tag{24}$$

$$u^s_3(x, \theta, t)|_{F_2} = \frac{F^s_2 L_s}{2\rho_s h_s N_{mn}} \sum_{m=1}^{\infty} \sum_{n=1}^{\infty} \frac{\cos n\theta^*_2}{(\omega^2_{mn} - \omega^2)} \sin(m\pi x/L_s) \cos n\theta e^{j\omega t}, \tag{25}$$

The circumferential slope of the shell can be obtained from equation (23) by differentiation with respect to the circumferential co-ordinate θ:

$$\psi^s_\theta(x, \theta, t) = \psi^s_\theta(x, \theta, t)|_{F_1} + \psi^s_\theta(\mathrm{x}, \theta, t)|_{F_2}, \tag{26}$$

where

$$\psi^s_\theta(x, \theta, t)|_{F_1} = -\frac{F^s_1 L_s}{2\rho_s h_s N_{mn}} \sum_{m=1}^{\infty} \sum_{n=1}^{\infty} \frac{n \cos n\theta^*_1}{(\omega^2_{mn} - \omega^2)} \sin(m\pi x/L_s) \sin n\theta e^{j\omega t}, \tag{27}$$

$$\psi^s_\theta(x, \theta, t)|_{F_2} = -\frac{F^s_2 L_s}{2\rho_s h_s N_{mn}} \sum_{m=1}^{\infty} \sum_{n=1}^{\infty} \frac{n \cos n\theta^*_2}{(\omega^2_{mn} - \omega^2)} \sin(m\pi x/L_s) \sin n\theta e^{j\omega t}. \tag{28}$$

As shown in Figure 3(b), the dynamic moment loading exerted at two joints due to the constraint by the plate can be expressed as

$$T_\theta = m^*_i(x, \theta^*, t) = M^s_i \sin(\bar{m}\pi x/L_s)\delta(\theta - \theta^*_i)e^{j\omega t}, \quad i = 1, 2, \tag{29}$$

where m^*_1, m^*_2 are the moment functions applied at two joints in the circumferential position, $\theta = \theta^*_1$ and θ^*_2 respectively. The forcing functions due to the moment loading can be obtained from reference [22] as

$$F^*_{mn} = \frac{1}{\rho h N_{mn}} \int_0^{2\pi} \int_0^{L_s} U_{3mn} \left[\frac{1}{a} \left\{ \frac{\partial(T_\theta)}{\partial\theta} \right\} \right] a \, dx \, d\theta. \tag{30}$$

Therefore, the displacement of the shell by moment loading can be expressed as

$$u^s_3(x, \theta, t) = u^s_3(x, \theta, t)|_{M_1} + u^s_3(x, \theta, t)|_{M_2}, \tag{31}$$

where

$$u^s_3(x, \theta, t)|_{M_1} = \frac{M^s_1 L_s}{2\rho_s h_s N_{mn}} \sum_{m=1}^{\infty} \sum_{n=1}^{\infty} \frac{n \cos n\theta^*_1}{(\omega^2_{mn} - \omega^2)} \sin(m\pi x/L_s) \cos n\theta e^{j\omega t}, \tag{32}$$

$$u^s_3(x, \theta, t)|_{M_2} = \frac{M^s_2 L_s}{2\rho_s h_s N_{mn}} \sum_{m=1}^{\infty} \sum_{n=1}^{\infty} \frac{n \cos n\theta^*_2}{(\omega^2_{mn} - \omega^2)} \sin(m\pi x/L_s) \cos n\theta e^{j\omega t}. \tag{33}$$

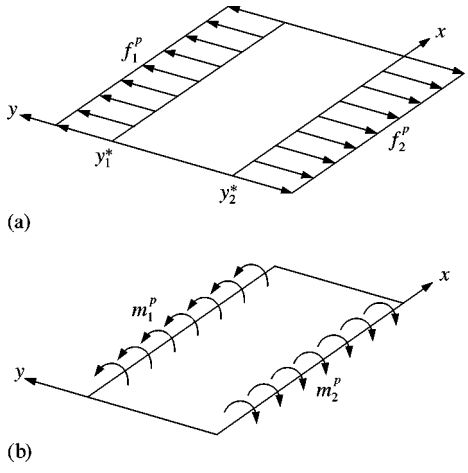

Figure 4. Forces (a) and moments (b) applied on the plate at the joints.

$u_3^s|_{M_1}$ is the displacement with only M_1 applied and $u_3^s|_{M_2}$ is the one with only M_2 applied. The slope of shell by moment loading at the joints can also be obtained from equation (23) by differentiation with respect to the circumferential co-ordinate θ.

$$\psi_\theta^s(x, \theta, t) = \psi_\theta^s(x, \theta, t)|_{M_1} + \psi_\theta^s(x, \theta, t)|_{M_2}, \tag{34}$$

where

$$\psi_\theta^s(x, \theta, t)|_{M_1} = -\frac{M_1^s L_s}{2\rho_s h_s N_{mn}} \sum_{m=1}^{\infty} \sum_{n=1}^{\infty} \frac{n^2 \cos n\theta_1^*}{(\omega_{mn}^2 - \omega^2)} \sin(m\pi x/L_s) \sin n\theta \, e^{j\omega t}, \tag{35}$$

$$\psi_\theta^s(x, \theta, t)|_{M_2} = -\frac{M_2^s L_s}{2\rho_s h_s N_{mn}} \sum_{m=1}^{\infty} \sum_{n=1}^{\infty} \frac{n^2 \cos n\theta_2^*}{(\omega_{mn}^2 - \omega^2)} \sin(m\pi x/L_s) \sin n\theta \, e^{j\omega t}. \tag{36}$$

As a similar method, one can consider the receptances for a rectangular plate simply supported at all edges with forces and moments exerted at two joints, (x, y_1^*) and (x, y_2^*). To formulate the receptances that one needs, the displacement and slope as the function of x-co-ordinate due to forces and moments are calculated. The dynamic excitation (Figure 4(a)) exerted at the joints due to the constraint of the displacements of the plate by the shell can be assumed as equation (37) using the Dirac delta and sinusoidal function.

$$f_i^*(x, y^*, t) = F_i^p \sin(\bar{m}\pi x/L_p)\delta(y - y_i^*)e^{j\omega t}, \quad i = 1, 2. \tag{37}$$

Also, the mode shape function expressing the in-plane displacement of the simply supported plate can be assumed as

$$U_{2mn}^p = \sin(m\pi x/L_p)\cos(n\pi y/b). \tag{38}$$

Thus, the displacement of the plate can be expressed as

$$u_2^p(x, y, t) = u_2^p(x, y, t)|_{F_1} - u_2^p(x, y, t)|_{F_2}, \tag{39}$$

where

$$u_2^p(x, y, t)|_{F_1} = \frac{2F_1^p}{\rho_p h_p b} \sum_{m=1}^{\infty} \sum_{n=1}^{\infty} \frac{\cos(n\pi y_1^*/b)}{(\omega_{mn}^2 - \omega^2)} \cos(n\pi y/b) \sin(m\pi x/L_p) e^{j\omega t}, \tag{40}$$

$$u_2^p(x, y, t)|_{F_2} = \frac{2F_2^p}{\rho_p h_p b} \sum_{m=1}^{\infty} \sum_{n=1}^{\infty} \frac{\cos(n\pi y_2^*/b)}{(\omega_{mn}^2 - \omega^2)} \cos(n\pi y/b) \sin(m\pi x/L_p) e^{j\omega t}. \tag{41}$$

To obtain the slope of a simply supported rectangular plate by edge moments, the transverse mode shape function given in equation (3) can be used. The periodic line moments (Figure 4(b)) excited at the joints, (x, y_1^*) and (x, y_2^*) can be expressed as

$$m_i^p(x, y^*, t) = M_i^p \sin(\bar{m}\pi x/L_p) \delta(y - y_i^*) e^{j\omega t}, \quad i = 1, 2. \tag{42}$$

Thus, the transverse displacement of the plate by dynamic moments is

$$u_3^p(x, y, t) = u_3^p(x, y, t)|_{M_1} - u_3^p(x, y, t)|_{M_2}, \tag{43}$$

where

$$u_3^p(x, y, t)|_{M_1} = -\frac{2\pi M_1^p}{\rho_p h_p b^2} \sum_{m=1}^{\infty} \sum_{n=1}^{\infty} \frac{n \cos(n\pi y_1^*/b)}{(\omega_{mn}^2 - \omega^2)} \sin(n\pi y/b) \sin(m\pi x/L_p) e^{j\omega t}, \tag{44}$$

$$u_3^p(x, y, t)|_{M_2} = -\frac{2\pi M_2^p}{\rho_p h_p b^2} \sum_{m=1}^{\infty} \sum_{n=1}^{\infty} \frac{n \cos(n\pi y_2^*/b)}{(\omega_{mn}^2 - \omega^2)} \sin(n\pi y/b) \sin(m\pi x/L_p) e^{j\omega t}. \tag{45}$$

The slope of the plate in the width direction by dynamic moments can be obtained from equation (43) by differentiation with respect to the co-ordinate, y:

$$\psi_2^p(x, y, t) = \psi_2^p(x, y, t)|_{M_1} - \psi_2^p(x, y, t)|_{M_2}, \tag{46}$$

where

$$\psi_2^p(x, y, t)|_{M_1} = -\frac{2\pi^2 M_1^p}{\rho_p h_p b^3} \sum_{m=1}^{\infty} \sum_{n=1}^{\infty} \frac{n^2 \cos(n\pi y_1^*/b)}{(\omega_{mn}^2 - \omega^2)} \cos(n\pi y/b) \sin(m\pi x/L_p) e^{j\omega t}, \tag{47}$$

$$\psi_3^p(x, y, t)|_{M_2} = -\frac{2\pi^2 M_2^p}{\rho_p h_p b^3} \sum_{m=1}^{\infty} \sum_{n=1}^{\infty} \frac{n^2 \cos(n\pi y_2^*/b)}{(\omega_{mn}^2 - \omega^2)} \cos(n\pi y/b) \sin(m\pi x/L_p) e^{j\omega t}. \tag{48}$$

2.3. FREQUENCY EQUATION FOR COMBINED SHELL

A receptance is defined as the ratio of a displacement or slope response at a certain point to a harmonic force or moment input at the same or different point. When the two systems are joined and no forces (or moments) external to the two systems are applied, it must be equal because of displacement (or slope) continuity. Thus, the natural frequencies of combined structure can be found from [22]

$$|\alpha_{ij} + \beta_{ij}| = 0, \tag{49}$$

where α_{ij} and β_{ij} are the receptance of the shell and the plate respectively.

For the combined shell with an interior rectangular plate as shown in Figure 2, receptances for the shell and the plate are defined as follows.

For the shell:

$$\alpha_{(2i-1)(2j-1)} = \frac{u^s_{3i}(x, \theta^*_i, t)|_{F_j}}{f_j}, \qquad \alpha_{(2i)(2j-1)} = \frac{\psi^s_{\theta i}(x, \theta^*_i, t)|_{F_j}}{f_j},$$

$$\alpha_{(2i-1)(2j)} = \frac{u^s_{3i}(x, \theta^*_i, t)|_{M_j}}{m_j}, \qquad \alpha_{(2i)(2j)} = \frac{\psi^s_{\theta i}(x, \theta^*_i, t)|_{M_i}}{m_j}, \quad i, j = 1, 2 \tag{50}$$

For the plate:

$$\beta_{(2i-1)(2j-1)} = \frac{u^p_{2i}(x, y^*_i, t)|_{F_j}}{(-1)^{(j-1)} f_j}, \qquad \beta_{(2i)(2j-1)} = \frac{\psi^p_{2i}(x, y^*_i, t)|_{F_j}}{(-1)^{(j-1)} f_j},$$

$$\beta_{(2i-1)(2j)} \sim \frac{u^p_{2i}(x, y^*_i, t)|_{M_j}}{(-1)^{(j-1)} m_j}, \qquad \beta_{(2i)(2j)} = \frac{\psi^p_{2i}(x, y^*_i, t)|_{M_j}}{(-1)^{(j-1)} m_j}, \quad i, j = 1, 2 \tag{51}$$

The frequency equation can be derived considering the continuity condition at shell/plate junctions. In this study, only the slope of the plate in the width direction and the normal displacement of the shell due to dynamic forces are considered. The normal displacement of the plate and the slope of the shell in the circumferential direction due to dynamic moments are taken into consideration because the other components of displacement can be ignored. By applying the continuity condition at the joints, the frequency equation can be expressed as

$$\begin{bmatrix} \alpha_{11}+\beta_{11} & \alpha_{12}+\beta_{12} & \alpha_{13}+\beta_{13} & \alpha_{14}+\beta_{14} \\ \alpha_{21}+\beta_{21} & \alpha_{22}+\beta_{22} & \alpha_{23}+\beta_{23} & \alpha_{24}+\beta_{24} \\ \alpha_{31}+\beta_{31} & \alpha_{32}+\beta_{32} & \alpha_{31}+\beta_{33} & \alpha_{34}+\beta_{34} \\ \alpha_{41}+\beta_{41} & \alpha_{42}+\beta_{42} & \alpha_{43}+\beta_{43} & \alpha_{44}+\beta_{44} \end{bmatrix} \begin{Bmatrix} F_1 \\ M_1 \\ F_2 \\ M_2 \end{Bmatrix} = 0. \tag{52}$$

For the rectangular plate, neglecting the in-plane displacements due to moments, (u^p_2/M) give $\beta_{12} = \beta_{14} = \beta_{32} = \beta_{34} = 0$. Similarly, the slopes in the normal direction due to forces (ψ^p_2/F) are also negligible, that is, $\beta_{21} = \beta_{23} = \beta_{41} = \beta_{43} = 0$. Thus, from the condition of having a non-trivial solution of equation (52), the frequency equation of the combined shell can be obtained in the following form.

$$\begin{vmatrix} \alpha_{11}+\beta_{11} & \alpha_{12} & \alpha_{13}+\beta_{13} & \alpha_{14} \\ \alpha_{21} & \alpha_{22}+\beta_{22} & \alpha_{23} & \alpha_{24}+\beta_{24} \\ \alpha_{31}+\beta_{31} & \alpha_{32} & \alpha_{31}+\beta_{33} & \alpha_{34} \\ \alpha_{41} & \alpha_{42}+\beta_{42} & \alpha_{43} & \alpha_{44}+\beta_{44} \end{vmatrix} = 0, \tag{53}$$

where α_{ij}, β_{ij} are the receptances of the shell and the plate respectively. They can be calculated as the ratio of a displacement (or slope) response at two joints to a harmonic force (or moment) input. The calculated receptances of the shell and the plate are given in Appendices A and B respectively.

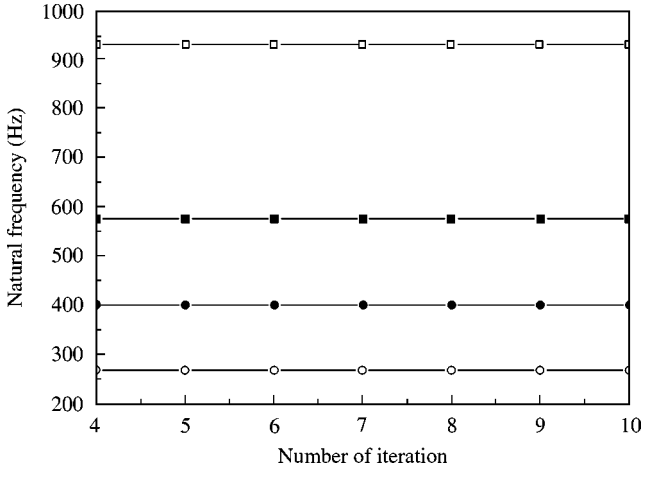

Figure 5. Convergence of frequencies for the CFRP plain weave composite combined shell with an interior plate at the center of the shell; $a = 0{\cdot}109$ m, $b = 0{\cdot}218$ m, $L_s = L_p = 0{\cdot}36$ m, $h_s = h_p = 0{\cdot}0037$ m, $E_1 = E_2 = 58{\cdot}0$ GPa, $G = 3{\cdot}9$ GPa, $\rho = 1540$ kg/m^3, $v = 0{\cdot}08$: —○—, plate only $P(1, 1)$; —●—, combined shell (first mode); —■—, combined shell (second mode); —□—, shell only $S(1, 3)$.

3. NUMERICAL RESULTS AND DISCUSSION

The frequencies of a combined shell are obtained by using a computer program. After finding the frequencies of the simply supported plate and shell at both ends, the results are used to calculate the natural frequencies of the combined shell. In order to examine the convergence of the natural frequencies obtained from the proposed method and determine the suitable terms of the iteration as the number of terms in the displacement series is increased, the natural frequencies for the experimental model which will be discussed later are estimated. In this case, the plate consisted of the same material and uniform thickness and length as the shell, and is located at the center of the shell. The results are shown in Figure 5. Subsequent analyses are made with at least 10 circumferential terms in the shell displacement series and seven terms in the plate displacement series.

To show the validity of the analytical results using the receptance method, the results are compared with those given by available references for a simply supported isotropic cylindrical shell with an interior plate at several locations. Following references, results are obtained for a shell of radius 0·254 m, length 1·27 m, and thickness 0·00508 m, with material properties $E = 200$ GPa, $\rho = 7500$ kg/m^3, and $v = 0{\cdot}3$. The interior plate is taken to have the same thickness and properties as the shell, and located at $\theta_1^* = 115^\circ$.

The natural frequencies are presented as frequency parameters, $\Omega = a\omega\sqrt{\rho(1 - v^2)/E}$, and are shown in Table 1. Peterson and Boyd [13] presented the results for the effects of a longitudinal, interior plate on the natural frequencies and mode shapes using a Rayleigh–Ritz technique. Missaoui *et al.* [17] studied the modal characteristics and the vibrational response of a cylindrical shell with a floor partition using artificial spring systems. It is shown that the present results using the receptance method are somewhat smaller than those of references [13, 17] for the symmetric and antisymmetric modes. But there is a good agreement (within 8·5%) between the present method and the reference's results. The fundamental frequency of the combined shell is 104·0 Hz and the normalized value is $\Omega = 0{\cdot}0306$. One can notice a clear deviation of the results obtained by Peterson *et al.* [13], particularly for the fundamental frequency. This is due to an error committed in

TABLE 1

Comparison of frequency parameters (Ω) *of the simply supported isotropic cylindrical shell with interior plate at* $\theta_1^* = 115^\circ$ *location;* $a = 0{\cdot}254$ m, $b = 0{\cdot}46$ m, $L_s = L_p = 1{\cdot}27$ m, $h_s = h_p = 0{\cdot}00508$ m

Mode	Frequency parameter (Ω)				
	Present method	Ref. [13]	Diff. (%)	Ref. [17]	Diff. (%)
1S	0·0306	0·0367	16·6	0·0334	8·4
2S	0·0670	0·0693	3·3	0·0715	6·3
3S	0·0883	0·0939	5·9	0·0958	7·8
4S	0·1128	0·1170	3·6	0·1150	1·9
1A	0·0589	0·0625	5·7	0·0606	2·8
2A	0·0774	0·0828	6·5	0·0805	3·8
3A	0·0961	0·1030	6·7	0·1050	8·4
4A	0·1277	0·1330	3·9	0·1330	3·9

TABLE 2

Comparison of frequency parameters (Ω) *of the simply supported isotropic cylindrical shell with interior plate* (*symmetric mode*) *at several locations;* $a = 0{\cdot}254$ m, $b = 0{\cdot}46$ m, $L_s = L_p = 1{\cdot}27$ m, $h_s = h_p = 0{\cdot}00508$ m

Plate location	Mode	Frequency parameter (Ω)				
		Present	Ref. [13]	Diff. (%)	Ref. [16]	Diff. (%)
$\theta_1^* = 90^\circ$	1	0·0255	0·0296	13·8	0·0267	8·4
	2	0·0670	0·0630	6·0	0·0647	6·3
	3	0·0791	0·0863	8·3	0·0855	7·8
	4	0·1368	0·1350	1·3	0·1320	1·9
$\theta_1^* = 115^\circ$	1	0·0306	0·0367	16·6	0·0321	4·7
	2	0·0670	0·0693	3·3	0·0713	6·0
	3	0·0883	0·0939	5·9	0·0949	6·9
	4	0·1128	0·1170	3·6	0·1160	2·7
$\theta_1^* = 135^\circ$	1	0·0491	0·0572	14·2	0·0483	1·6
	2	0·0670	0·0709	4·2	0·0707	5·2
	3	0·0775	0·0795	2·5	0·0818	5·3
	4	0·1377	0·1330	3·4	0·1360	1·2

the compatibility equations at the floor/shell junctions in his work, which has also been pointed out and criticized by Langley [16] and Missaoui *et al.* [17].

Table 2 presents the frequency parameters of the symmetric modes of a cylindrical combined shell with an interior plate at several locations, $\theta_1^* = 90$, 115, and 135°. The comparison of results is made with those given by Peterson *et al.* [13], and Langley [16] using a dynamic stiffness technique. The fundamental frequency of the combined shell

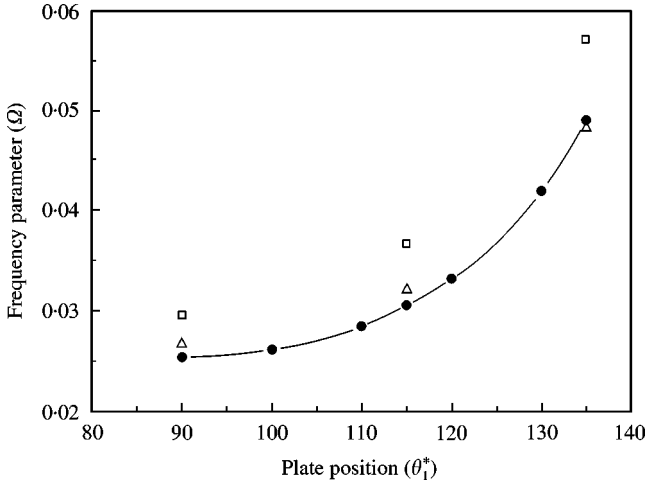

Figure 6. Comparison of fundamental frequency parameters (Ω) of the isotropic cylindrical shell with an interior plate of several locations: —●—, present; □, reference [13]; △, reference [16].

TABLE 3

Dimensions (mm) of CFRP plain weave composite combined shells

Plate location	Shell			Plate		
	Length (L_s)	Radius (a)	Thickness (h_s)	Length (L_p)	width (b)	Thickness (h_p)
$\theta_1^* = 90^\circ$	360	109	3·7	360	218	3·7
$\theta_1^* = 120^\circ$	360	109	4·0	360	188·8	3·6

increases as the plate is located farther from the center of the shell. Since the first mode of the combined shell involves only bending of the interior plate, this increment can be attributed to a decrease in the width of the plate. The results for mode shapes may be found in references and experimental values, which will be discussed in Figures 7 and 8. As a result, the present results agree well (within 8·5%), except for a clear deviation of the fundamental frequency given by reference [13]. This trend can also be confirmed from the results as shown in Figure 6, which provide the comparison of the fundamental frequency parameter to various locations of the plate.

As another method to verify the analytical results, a modal test using the impact exciting method is performed. The specimens manufactured in this investigation are composed of CFRP plain weave composite with stacking sequence, $[0_3/\pm 45_3/90_3^\circ]_s$. The geometrical data of the combined shells tested are given in Table 3. The shells consist of the same material and length as the plate. The plate is attached at $\theta_1^* = 90$ and 120° locations on the shell and fabricated by co-curing in an autoclave. The material properties of the CFRP composite specimen are obtained by uniaxial tensile tests as

$$E_1 = E_2 = 58{\cdot}0\ \text{GPa}, \quad G_{12} = 3{\cdot}9\ \text{GPa}, \quad \rho = 1540\ \text{kg/m}^3, \quad \nu_{12} = 0{\cdot}08$$

TABLE 4

Comparison of the natural frequencies of analytical and experimental results of the CFRP plain weave composite cylindrical shell with an interior plate at $\theta_1^* = 90^\circ$ location

	Method			
		Experiment		
Mode†	Receptance Freq. (Hz)	Freq. (Hz)	$P(m, n)$	$S(m, n)$
First	389·6	400·0	(1, 1)	—
Second	568·2	575·0	(2, 1)	—
Third	905·0	887·5	(3, 1)	—
Fourth	925·7	925·0	(1, 2)	—
Fifth	1162·6	987·5	(1, 2)	(1, 3)
Sixth	1250·8	1225·0	(2, 2)	—
Seventh	1284·9	1262.5	—	(1, 2)
Eighth	1333·9	1325·0	—	(1, 4)
Ninth	1399·5	1512·0	(3, 2)	(1, 4)
Tenth	1644.8	1650·0	—	(1, 5)

†Frequency ascending order.

Note: (1) A dash and underline indicate small amplitude. (2) $P(m, n)$, $S(m, n)$: Half wave numbers of the plate and shell.

The first 10 natural frequencies (Hz) of analytical and experimental methods of CFRP plain weave composite cylindrical shell with an interior plate at the center of the shell ($\theta_1^* = 90^\circ$) are listed in Table 4. In the table, a dash and underline of the experimental results indicate small amplitude, and the $P(m, n)$ and $S(m, n)$ represent the mode numbers of the plate and shell respectively. m represents the longitudinal wave number, and n represents the width or circumferential wave numbers. The discrepancy between analytical and experimental results is about 2·6% for the lowest fundamental frequency, and less than 7·5% for the other frequencies, except for the fifth mode coupled between the plate and the shell with a maximum 15% difference. When the plate is attached at the center of the shell, the interior plate greatly restricts the behavior of the shell, which first appears in the fifth mode. Among many causes of the deviation between analytical and experimental results, the 15% deviation in the fifth mode is due to the effect of boundary conditions on the natural frequencies in the experiment. The fundamental frequency of the combined shell is 389·6 Hz, and it shows the first bending mode of the interior plate with one half longitudinal and width weave, $P(1, 1)$. As shown in the table, the first three frequencies are the bending modes ($m = 1, 2, 3$) of the plate in the longitudinal direction for $n = 1$. This is because the length (L_p) of the plate is larger than the width (b). The fourth frequency is $P(1, 2)$ mode, which shows the second bending of an interior plate in the width direction. For the specimen considered in this study, the first frequency of the shell appears in the fifth mode as an ascending order, and it is 1162·6 Hz with the $S(1, 3)$ mode. Generally, in the case of the same dimension between the plate and the shell, the stiffness of the shell is greater than that of the plate. Thus, the frequency showing the shell mode is also higher than for the plate because the frequencies of the combined shell depend on the vibrational characteristics before combination of the two systems.

Table 5 presents the natural frequencies (Hz) of the CFRP combined shell with an interior plate at $\theta_1^* = 120^\circ$ location. Although the thickness of the two specimens shows little difference, the characteristics similar to the results provided in Table 4 are observed

TABLE 5

Comparison of the natural frequencies of analytical and experimental results of the CFRP plain weave composite cylindrical shell with an interior plate at $\theta_1^* = 120^\circ$ location

	Method			
		Experiment		
Mode†	Freq. (Hz) Receptance	Freq. (Hz)	$P(m, n)$	$S(m, n)$
First	476·4	470·0	(1, 2)	—
Second	644·0	620·0	(2, 1)	—
Third	963.1	865·0	(3, 1)	—
Fourth	973·4	925·0	(1, 2)	(1, 3)
Fifth	1082·8	1080·0	(4, 1)	(1, 2)
Sixth	1210·6	1215·0	—	(1, 4)
Seventh	1268·2	1305·0	(1, 3)	—
Eighth	1389·8	1340·0	—	(1, 4)
Ninth	1437·2	1430·0	(2, 2)	—
Tenth	1451.2	1660·0	(3, 2)	—

†Frequency ascending order.

on the natural frequencies and modes. When the plate is located farther from the center of the shell, the first three frequencies are increased because the plate modes are dominant in the lower frequencies. This phenomenon can be recognized as the stiffness effect of the plate due to the decrement of the width acting on the frequency of the combined shell. It can be found that the first frequency of the shell appears in the fourth mode, $S(1, 3)$.

The experimental mode shapes of CFRP combined cylindrical shell with the plate at $\theta_1^* = 90^\circ$ and 120° locations are shown in Figures 7 and 8. These figures show a cross-section of the combined shell in the longitudinal and circumferential directions. As obtained by previous workers and experimental results, the lowest frequency corresponds to a bending mode, which is basically governed by an interior plate motion. In case of the combined shell with the plate at the center of the shell the first four frequencies show the transverse bending modes of an interior plate with negligible motion of the shell. The shell mode appears first in the fifth mode, in which one notices a slight deformation of the plate and a strong motion of the shell.

Figure 8 shows the experimental mode shapes of a combined shell with the plate located farther from the center of the shell ($\theta_1^* = 120^\circ$) than in the case discussed in Figure 7 ($\theta_1^* = 90^\circ$). In this case the same trends are noted for the modes of an interior plate. However, the circumferential bending of the shell and the transverse bending of the plate are coupled with the increment of the frequency, especially for the $S(1, 2)$ mode of the shell.

4. CONCLUSIONS

A frequency equation for the analysis of free vibration of the circular cylindrical shell with an interior plate is formulated using the receptance method. Using the analysis results of free vibration for two simply supported structures by Love's shell and classical plate theory,

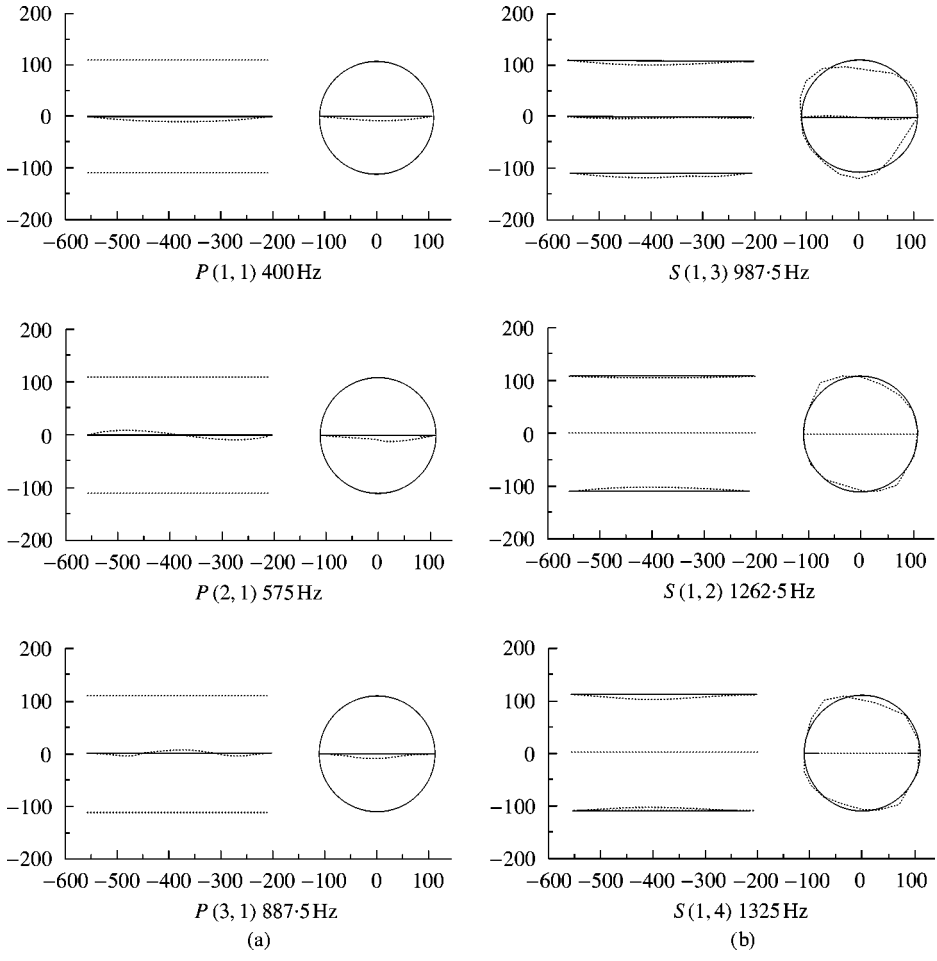

Figure 7. Experimental mode shapes of the CFRP plain weave composite cylindrical shell with an interior plate at $\theta_*^1 = 90^\circ$ location: (a) plate modes and (b) shell modes.

a frequency equation of the shell/plate combined system was obtained. The natural frequencies are compared with the previously published and experimental results to show the validity of the current formulation. The main conclusions of the investigations are summarized as follows.

(1) When the line load and moment applied along the joint are assumed as sinusoidal function, the continuity conditions at the plate/shell joints are proven to be satisfied.

(2) The fundamental frequency of the combined shell exhibits principally plate motion with one half wave in each direction. As the effect of the location of the plate, the frequencies for the lower range showing plate modes increase as the plate is located farther from the center of the shell due to the increment of the plate stiffness.

(3) For the combined system, the dominant frequency of the shell appears in the fourth or fifth mode due to the stiffness difference between the plate and the shell.

(4) It is expected that the method developed in this paper can be used for the analysis of free vibration of the combined cylindrical shell with arbitary end conditions.

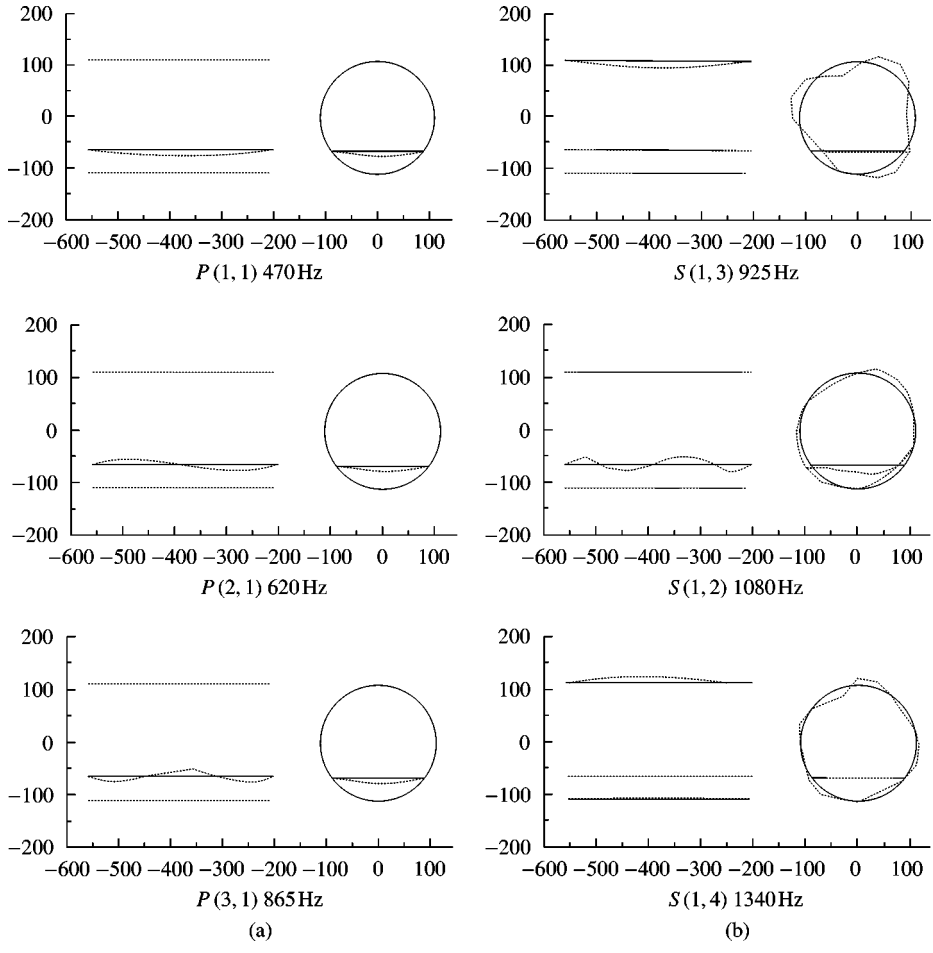

Figure 8. Experimental mode shapes of the CFRP plain weave composite cylindrical shell with an interior plate at $\theta_*^1 = 120^\circ$ location: (a) plate modes and (b) shell modes.

REFERENCES

1. A. W. Leissa 1973 *NASA SP*-228. U.S. Government Printing Office, Washington, DC. Vibration of shells.
2. A. W. Leissa 1973 *Journal of Sound and Vibration* **31**, 257–293. The free vibration of rectangular plates.
3. J. L. Sewall and E. C. Naumann 1968 *NASA TN*, *D*-4705. An experimental and analytical vibration study of thin shells with and without longitudinal stiffeners.
4. J. L. Sewall, W. M. Thompson and C. G. Pusey 1971 *NASA TN*, *D*-6089. An experimental and analytical vibration study of elliptical cylindrical shells.
5. Y. S. Lee and Y. W. Kim 1998 *Computers and Structures* **69**, 271–281. Vibration analysis of the rotating composite cylindrical shells with orthogonal stiffeners.
6. Y. S. Lee and Y. W. Kim 1999 *Advances in Engineering Software* **30**, 649–655. The effects of boundary conditions on the natural frequencies for the rotating composite cylindrical shells with orthogonal stiffeners.
7. R. E. D. Bishop and D. C. Johnson 1960 *The Mechanics of Vibration*. London: Cambridge University Press.

8. I. E. SHKAROV 1962 *NASA Technical Translation F*-341, 797–805. Use of the method of dynamic rigidities for calculating the frequencies of natural vibrations of built-up shells.
9. S. AZIMI, J. F. HAMILTON and W. SOEDEL 1984 *Journal of Sound and Vibration* **93**, 9–29. The receptance method applied to the free vibration of continuous rectangular plates.
10. S. AZIMI, J. F. HAMILTON and W. SOEDEL 1986 *Journal of Sound and Vibration* **109**, 79–88. Natural frequencies and modes of cylindrical polygonal ducts using receptance methods.
11. D. T. HUANG and W. SOEDEL 1993 *Journal of Sound and Vibration* **163**, 403–427. Natural frequencies and mode shapes of a circular plate welded to a circular cylindrical shell at arbitrary axial positions.
12. J. S. YIM, D. S. SHON and Y. S. LEE 1998 *Journal of Sound and Vibration* **213**, 75–88. Free vibration of clamped–free circular cylindrical shell with a plate attached at an arbitrary axial position.
13. M. R. PETERSON and D. E. BOYD 1978 *Journal of Sound and Vibration* **60**, 45–62. Free vibrations of circular cylinders with longitudinal, interior partitions.
14. T. IRIE, G. YAMADA and Y. KOBAYASHI 1984 *Journal of Sound and Vibration* **96**, 133–142. Free vibration of non-circular cylindrical shells with longitudinal interior partitions.
15. T. IRIE and G. YAMADA 1984 *Journal of Sound and Vibration* **95**, 31–39. Free vibration of jointed conical–cylindrical shells.
16. R. S. LANGLEY 1992 *Journal of Sound and Vibration* **156**, 521–540. A dynamic stiffness technique for the vibration analysis of stiffened shell structures.
17. J. MISSAOUI, L. CHENG and M. J. RICHARD 1995 *Journal of Sound and Vibration* **190**, 21–40. Free and forced vibration of a cylindrical shell with a floor partition.
18. M. PETYT and J. WEI 1997 *Proceeding of the* 15*th International Modal Analysis Conference*, *Japan*, 647–653. Free vibration of an idealized fuselage structure.
19. D. J. EWINS 1984 *Modal Testing*: *Theory and Practice*. New York: John Wiley & Sons, Inc.
20. J. M. WHITNEY 1987 *Structural Analysis of Laminated Anisotropic Plates*. Lancaster, PA: Technomic Publishing Co.
21. R. M. JONES 1975 *Mechanics of Composite Material*. New York: Hemisphere Publishing Co.
22. W. SOEDEL 1993 *Vibrations of Shells and Plates*. Hong Kong: Marcel Dekker.

APPENDIX A: TERMS IN EQUATION (53)

In equation (53) the receptances of the shell are given as

$$\alpha_{11}=\frac{u^s_{31}(x,\theta_1^*,t)|_{F_1}}{f_1^s}=\frac{(F_1^s L_s/2\rho_s h_s N_{mn})\sum_{m=1}^{\infty}\sum_{n=1}^{\infty}(\cos n\theta_1^*/(\omega_{mn}^2-\omega^2))\sin(m\pi x/L_s)\cos n\theta e^{j\omega t}}{F_1^s\sin(\bar{m}\pi x/L_s)e^{j\omega t}} \tag{A1}$$

$$= SRC\cos n\theta_1^*\cos n\theta_1^*,$$

where if one lets

$$SRC=\frac{L_s}{2\rho_s h_s N_{mn}}\sum_{m=1}^{\infty}\sum_{n=1}^{\infty}\frac{1}{(\omega_{mn}^2-\omega^2)},$$

$$\alpha_{31}=\frac{u^s_{32}(x,\theta_2^*,t)|_{F_1}}{f_1^s}=SRC\cos n\theta_1^*\cos n\theta_2^*, \tag{A2}$$

$$\alpha_{13}=\frac{u^s_{31}(x,\theta_1^*,t)|_{F_2}}{f_2^s}=SRC\cos n\theta_1^*\cos n\theta_2^*, \tag{A3}$$

$$\alpha_{33}=\frac{u^s_{32}(x,\theta_2^*,t)|_{F_2}}{f_2^s}=SRC\cos n\theta_2^*\cos n\theta_2^*, \tag{A4}$$

$$\alpha_{21} = \frac{\psi^s_{\theta 1}(x, \theta^*_1, t)|_{F_1}}{f^s_1} = -SRC\, n \cos n\theta^*_1 \sin n\theta^*_1, \tag{A5}$$

$$\alpha_{41} = \frac{\psi^s_{\theta 2}(x, \theta^*_2, t)|_{F_1}}{f^s_1} = -SRC\, n \cos n\theta^*_1 \sin n\theta^*_2, \tag{A6}$$

$$\alpha_{23} = \frac{\psi^s_{\theta 1}(x, \theta^*_1, t)|_{F_2}}{f^s_2} = -SRC\, n \cos n\theta^*_2 \sin n\theta^*_1, \tag{A7}$$

$$\alpha_{43} = \frac{\psi^s_{\theta 2}(x, \theta^*_2, t)|_{F_2}}{f^s_2} = -SRC\, n \cos n\theta^*_2 \sin n\theta^*_2, \tag{A8}$$

$$\alpha_{12} = \frac{u^s_{31}(x, \theta^*_1, t)|_{M_1}}{m^s_1} = SRC\, n \sin n\theta^*_1 \cos n\theta^*_1, \tag{A9}$$

$$\alpha_{32} = \frac{u^s_{32}(x, \theta^*_2, t)|_{M_1}}{m^s_1} = SRC\, n \sin n\theta^*_1 \cos n\theta^*_2, \tag{A10}$$

$$\alpha_{14} = \frac{u^s_{31}(x, \theta^*_1, t)|_{M_2}}{m^s_2} = SRC\, n \sin n\theta^*_2 \cos n\theta^*_1, \tag{A11}$$

$$\alpha_{34} = \frac{u^s_{32}(x, \theta^*_2, t)|_{M_2}}{m^s_2} = SRC\, n \sin n\theta^*_2 \cos n\theta^*_2, \tag{A12}$$

$$\alpha_{22} = \frac{\psi^s_{\theta 1}(x, \theta^*_1, t)|_{M_1}}{m^s_1} = -SRC\, n^2 \sin n\theta^*_1 \sin n\theta^*_1, \tag{A13}$$

$$\alpha_{42} = \frac{\psi^s_{\theta 2}(x, \theta^*_2, t)|_{M_1}}{m^s_1} = -SRC\, n^2 \sin n\theta^*_1 \sin n\theta^*_2, \tag{A14}$$

$$\alpha_{24} = \frac{\psi^s_{\theta 1}(x, \theta^*_1, t)|_{M_2}}{m^s_2} = -SRC\, n^2 \sin n\theta^*_2 \sin n\theta^*_1, \tag{A15}$$

$$\alpha_{44} = \frac{\psi^s_{\theta 2}(x, \theta^*_2, t)|_{M_2}}{m^s_2} = -SRC\, n^2 \sin n\theta^*_2 \sin n\theta^*_2. \tag{A16}$$

APPENDIX B: TERMS IN EQUATION (53)

Similarly, in equation (53) the receptances of the plate are given as:

$$\beta_{11} = \frac{u^p_{21}(x, y^*_1, t)|_{F_1}}{f^p_1} = \frac{(2F^p_1/\rho_p h_p b) \sum_{m=1}^{\infty} \sum_{n=1}^{\infty} (\cos(n\pi y^*_1/b)/(\omega^2_{mn} - \omega^2)) \cos(n\pi y/b) \sin(m\pi x/L_p) e^{j\omega t}}{F^p_1 \sin(\bar{m}\pi x/L_p) e^{j\omega t}}$$

$$= -\frac{2}{\rho_p h_p b \omega^2}, \tag{B1}$$

$$\beta_{31} = \frac{u^p_{22}(x, y^*_2, t)|_{F_1}}{f^p_1} = \frac{2}{\rho_p h_p b \omega^2}, \tag{B2}$$

$$\beta_{13} = \frac{u_{21}^p(x, y_1^*, t)|_{F_2}}{f_2^p} = -\frac{2}{\rho_p h_p b \omega^2}, \tag{B3}$$

$$\beta_{33} = \frac{u_{22}^p(x, y_2^*, t)|_{F_2}}{f_2^p} = \frac{2}{\rho_p h_p b \omega^2}, \tag{B4}$$

$$\beta_{22} = \frac{\psi_{21}^p(x, y_1^*, t)|_{M_1}}{m_1^p} = -\frac{2\pi^2}{\rho_p h_p b^3} \sum_{m=1}^{\infty} \sum_{n=1}^{\infty} \frac{n^2}{(\omega_{mn}^2 - \omega^2)}, \tag{B5}$$

$$\beta_{42} = \frac{\psi_{22}^p(x, y_2^*, t)|_{M_1}}{m_1^p} = \frac{2\pi^2}{\rho_p h_p b^3} \sum_{m=1}^{\infty} \sum_{n=1}^{\infty} \frac{n^2}{(\omega_{mn}^2 - \omega^2)}, \tag{B6}$$

$$\beta_{24} = \frac{\psi_{21}^p(x, y_1^*, t)|_{M_2}}{m_2^p} = -\frac{2\pi^2}{\rho_p h_p b^3} \sum_{m=1}^{\infty} \sum_{n=1}^{\infty} \frac{n^2}{(\omega_{mn}^2 - \omega^2)}, \tag{B7}$$

$$\beta_{44} = -\frac{\psi_{22}^p(x, y_2^*, t)|_{M_2}}{m_2^p} = \frac{2\pi^2}{\rho_p h_p b^3} \sum_{m=1}^{\infty} \sum_{n=1}^{\infty} \frac{n^2}{(\omega_{mn}^2 - \omega^2)}. \tag{B8}$$

APPENDIX C: NOMENCLATURE

A_{ij}	extensional stiffness of shell ($i, j = 1, 2, 6$)
a	radius of the shell
b	width of the plate
D_{ij}	bending stiffness of the plate and shell ($i, j = 1, 2, 6$)
E_1, E_2	Young's modulus in the axial and transverse direction
f_i, F_i	forces and amplitudes at shell/plate junction in the transverse or width directions
F_{mn}^*	dynamic force function
G_{12}	shear modulus
h_p, h_s	thickness of the plate, shell
k_{ij}	stiffness matrix of the shell ($i, j = 1, 2, 3$)
L_p, L_s	length of the plate, shell
m_i, M_i	moments and amplitudes at shell/plate junction ($i = 1, 2$)
m_{ij}	mass matrix of the shell ($i, j = 1, 2, 3$)
q_i^*	input forcing functions at shell/plate junction in the axial, circumferential and transverse normal to the surface ($i = 1, 2, 3$)
T_θ	line moments at shell/plate junction
u_i^s	displacement components of the shell in the axial, circumferential and transverse direction ($i = 1, 2, 3$)
u_i^p	displacement components of the plate in the axial, width and transverse direction ($i = 1, 2, 3$)
U_{ik}	natural mode components in each direction for mode mn ($i = 1, 2, 3$)
x, y, z_p	co-ordinates of the plate
x, θ, z_s	co-ordinates of the shell
y_1^*, y_2^*	y directional co-ordinates of the plate where the shell is attached
α_{ij}, β_{ij}	receptances of the shell and plate ($i, j = 1, 2, 3, 4$)
δ	Dirac delta function
$\varepsilon_x, \varepsilon_\theta, \varepsilon_{x\theta}$	strains of the shell mid-surface
ζ_{mn}	modal damping coefficient
η_{mn}	modal participation factor of mode mn
θ_1^*, θ_2^*	circumferential co-ordinates of the shell where the plate is attached
$\kappa_x, \kappa_\theta, \kappa_{x\theta}$	curvatures of the shell mid-surface
ρ_p, ρ_s	mass density of the plate and shell
ψ_2^p	slope of the plate in the width direction
ψ_θ^s	slope of the shell in the circumferential direction
Ω	non-dimensional frequency parameter, $a\omega\sqrt{\rho(1 - \nu^2/E}$

ω angular frequency of the combined shell for mode mn
ω_{mn} angular frequency of the plate and shell for (m, n) mode

Superscripts or subscripts

s cylindrical shell
p rectangular plate
mn mnth mode
F_1, F_2 forces applied at shell/plate junctions, $\theta = \theta_1^*$ and θ_2^* respectively
M_1, M_2 moments applied at shell/plate junctions, $\theta = \theta_1^*$ and θ_2^* respectively